Cellular and Molecular Bioengineering, Vol. 7, No. 4, December 2014 (© 2014) pp. 497–509
DOI: 10.1007/s12195-014-0362-7

Multistage Adipose-Derived Stem Cell Myogenesis: An Experimental and Modeling Study

PINAR YILGOR HURI,[1,2] ANDREW WANG,[1] ALEXANDER A. SPECTOR,[1] and WARREN L. GRAYSON[1,2]

[1]Department of Biomedical Engineering, Johns Hopkins University School of Medicine, Baltimore, MD 21287, USA; and [2]Translational Tissue Engineering Center, Johns Hopkins University School of Medicine, Baltimore, MD 21231, USA

(*Received 17 June 2014; accepted 4 October 2014; published online 15 October 2014*)

Associate Editor Michael R. King oversaw the review of this article.

Abstract—Adipose-derived stem/stromal cells (ASCs) possess great potential as an autologous cell source for cell-based regenerative therapies. We have previously shown that mimicking the natural dynamic muscle loading patterns enhances differentiation capacity of ASCs into aligned myotubes. In particular, the application of uniaxial cyclic strain significantly increased ASC myogenesis in monolayer cultures. In this study, we demonstrate that the temporal expression of key myogenic markers Pax3/7, Desmin, MyoD and myosin heavy chain closely mimics patterns described for muscle satellite cells. Using these lineage markers, we propose that the progression from undifferentiated ASCs to myotubes can be described as transitions through discrete stages. Based on our experimental data, we developed a compartmental kinetic stage-transition model to provide a quantitative description of the differentiation of ASCs to terminally differentiated myotubes. The model describing ASCs' myogenic differentiation in response to biophysical cues could help to obtain a deeper understanding of factors governing the biological responses and provide clues for experimental methods to increase the efficiency of ASC myogenesis for the development of improved muscle regenerative therapies.

Keywords—Adipose-derived stem cell, Myogenesis, Dynamic culture, Uniaxial strain, Kinetic stage-transition model.

INTRODUCTION

Upon injury, skeletal muscle has a robust capacity for spontaneous regeneration, which is mediated by the activation of normally quiescent satellite cells. Activated satellite cells divide asymmetrically, giving rise to myoblasts and more satellite cells to replenish the progenitor-cell pool.[18] Their proliferation, differentiation into myoblasts, alignment, and fusion into existing myotubes to form multinucleated muscle fibers is highly orchestrated[34] and can be defined by the sequential expression of key transcription factors and cytoskeletal proteins. For example, quiescent satellite cells express Pax3 and Pax7 which are important in the specification of progenitor cells to satellite cell lineage during embryogenesis.[35] Upon injury, activated satellite cells express Pax7 and MyoD. Pax7 expression is ultimately downregulated while the expression of myoD is maintained. Subsequently, myf5 is turned on and, together with myoD, leads to terminal differentiation into myoblasts.[17] Satelite cell-derived primary myoblasts have been shown to express MyoD, Myf5, Pax7, and Desmin.[1] Myoblasts that have terminally differentiated into myotubes express myogenin, muscle creatine kinase and the structural protein, myosin heavy chain (MHC).[33]

Although they play a vital role during muscle development and repair, recent studies have shown that satellite cells are not the only myogenic precursors. Progenitor cells isolated from muscle, neuronal compartment, and various mesenchymal tissues including bone marrow and adipose tissue possess myogenic capacities.[11,12,21,27,32] Among these, adipose-derived stem/stromal cells (ASCs) are a very clinically relevant cell source for muscle regenerative therapies due to relative ease of procurement, low morbidity, and demonstrated myogenic potential. ASCs differentiate into myoblasts upon chemical induction when cultured on softer substrates that mimic the stiffness of native muscle ECM.[10] We previously demonstrated enhanced differentiation efficiency by mimicking physiological loading profiles (i.e., applying uniaxial cyclic stretch to the cells).[37] Such an effect was also observed in primary human myoblast cultures, where cyclic strain enhanced myofiber diameter and area as compared to static culture.[30] Several other studies have also explored the effect of

Address correspondence to Warren L. Grayson, Department of Biomedical Engineering, Johns Hopkins University School of Medicine, Baltimore, MD 21287, USA. Electronic mail: wgrayson@jhmi.edu

mechanical loading on stem cell myogenesis. For example, enhanced vascular smooth muscle marker expression and decreased proliferation rate was reported for ASCs upon 10% uniaxial cyclic strain.[20] In another study, rat bone marrow mesenchymal stem cells (MSCs) expressed higher level of smooth muscle markers with increased frequency of cyclic stretch.[25] These studies suggest that a more fundamental understanding of the factors governing cellular reprogramming could lead to the development of techniques to enhance the myogenic differentiation capacity of ASCs. Based on the results of our previous study which demonstrated enhanced alignment and MHC expression of ASCs on day 21 of dynamic culture, the goals of this study were to: (1) gain a deeper insight into the kinetics of ASC myogenesis in response to biochemical and biophysical induction by assessing: (i) the expression profiles of 4 different myogenic markers (Pax3/7, MyoD1, Desmin and MHC) throughout the dynamic and static culture (days 1, 3, 7, 14 and 21), and (ii) cell proliferation patterns during this process and (2) Use this data to develop a computational model that describes this process.

Computational modeling has been successfully applied to aid understanding of lineage progression pathways during stem cell differentiation in response to various environmental cues.[22,36] Multistage "static"[7] and "dynamic"[24] models have been applied to hematopoietic stem cells (HSCs) to assess the cell population under normal (healthy) and diseased (cancer) conditions. The kinetic model characterizing HSC differentiation postulated multiple intermediate phenotypic stages and, so doing, revealed critical insight into possible feedback mechanisms governing cell proliferation and differentiation that aided in the interpretation of experimental data. Other reports of modeling HSC differentiation revealed the importance of a threshold value of soluble factors in HSC expansion (such as interleukin-3 and transforming growth factor-β) and ligand-receptor interactions to enhance the probability of differentiation.[38] In spite of its success, kinetic, multi-stage models have not previously been applied to adherent mesenchymal stem cell (MSC) or ASC populations as the stages of progression along distinct mesenchymal lineages (e.g., osteoblasts, chondrocytes, and/or adipocytes) have not been precisely defined in terms of discrete, intermediate steps.

In this study, we used combined experimental and modeling approaches to study ASC myogenesis. We have shown that in response to synergistic biochemical and biophysical stimulation, ASCs express myogenic markers following a defined temporal sequence. Based on the experimentally determined markers and their specific expression profiles (Pax 3/7, MyoD, Desmin and MHC), we defined discrete stages and developed a kinetic stage-transition model to describe the ASC myogenesis in silico for the first time in the literature.

METHODS

Isolation and Culture of ASCs

ASCs were isolated at the Stem Cell Biology Laboratory, Pennington Biomedical Research Center, under an Institutional Review Board approved protocol (PBRC #23040) according to published methods.[9] Briefly, fresh human subcutaneous adipose lipoaspirates were obtained under informed consent from healthy Caucasian female donors undergoing elective liposuction surgery with a mean age of 47.6 ± 1.9 years and mean body mass index of 27.1 ± 0.6. The lipoaspirate tissue was extensively washed with warm phosphate buffer solution (PBS) to remove erythrocytes and then digested in PBS supplemented with 0.1% Collagenase Type I (Worthington Biochemical Corp.), 1% BSA, and 2 mM $CaCl_2$ for 1 h at 37 °C. Following room temperature centrifugation at 300 g and resuspension in Stromal Medium (DMEM/Hams F-12 Medium supplemented with 10% FBS (Hyclone), 100 U/mL penicillin, 100 μg/mL streptomycin, and 0.25 μg/mL Amphotericin B (Fisher Scientific)), the stromal vascular pellet obtained from 35 mL of lipoaspirate digest was plated in a T175 flask (0.2 mL per cm^2). The adherent cells were washed with warm PBS one day after plating and maintained in Stromal Medium until 80–90% confluency. The adherent population ("passage 0") was harvested by digestion with trypsin (0.05%)/EDTA (1 mM) at 37 °C for 5 min, washed with Stromal Medium and cryopreserved[14] for shipment to Johns Hopkins University. Prior studies have demonstrated no deleterious effects—such as loss of multipotency—on ASCs due to cryopreservation.[14,15,23] For expansion, ASCs were thawed and cultured in expansion medium: high-glucose DMEM (GIBCO Invitrogen) with 10% fetal bovine serum (FBS; Atlanta Biologicals), 1% penicillin/streptomycin (P/S, GIBCO Invitrogen), and 1 ng/mL FGF-2 (PeproTech). Cells were cultured in culture medium (CM) containing low-glucose DMEM (GIBCO Invitrogen) with 10% FBS, 1% P/S and 1 ng/mL FGF-2[16] after seeding for further experiments for 21 days except for the period of myogenic induction.

Myogenic Induction of ASCs

Passage 2 ASCs were seeded at 5000 cells/cm^2 in collagen I coated 6-well plates with flexible membrane substrates (UniFlex Culture Plate, Flexcell International

Corp). Biochemical stimulation was done 24 h after seeding *via* myogenic induction medium composed of low-glucose DMEM supplemented with 1% FBS, 5% horse serum (Invitrogen), 10 μM 5-Azacytidine (Sigma) and 1% P/S.[37] After 24 h, the wells were washed with PBS and fed with fresh CM for the rest of the culture. ASCs were either grown in *Static* or *Dynamic* conditions on the flexible membranes. *Dynamic* cultures were exposed to uniaxial cyclic strain using the Flexcell system (FX-5000^{TM}) between days 3–21 of culture (10% strain, 0.5 Hz, 1 h/day). *Static* controls were not subjected to strain.

Determination of Viable Cell Number

Alamar Blue assay (US Biological) was used to determine the number of metabolically active (live) cells during culture. Briefly, Alamar Blue solution (10%, 1 mL) in colorless DMEM (GIBCO Invitrogen) was added to the wells after washing with PBS and incubating at 37 °C and 5% CO_2 for 1 h. Then, 200 μL of the test solution was transferred to a 96-well plate and absorbance was determined at 570 and 595 nm using the plate reader. The test medium in the wells was then discarded, washed with PBS, fresh CM was added to the wells to continue cell culture. Percent reduction of the Alamar blue dye was correlated to viable cell number through a calibration curve.

Identification of Proliferating Cells

Bromodeoxyuridine (BrdU, Sigma) incorporation was performed in order to identify the proliferating cells in culture. For this, 10 μm BrdU was added to the culture medium for 18 h. Afterwards, the wells were rinsed with PBS and fixed with paraformaldehyde for 20 min. DNA was denatured by incubating cells with 2 N HCl in 0.5% triton-X-100 in dI water for 30 min. After extensive washing, samples were blocked with 5% mouse serum in PBS for 30 min, followed by overnight incubation with mouse anti-BrdU conjugated to Alexa Fluor®647 (1:50, Invitrogen) at 4 °C. The nuclei were then counterstained with DAPI for 10 min. The samples were mounted in 50% glycerol in PBS and imaged using Zeiss Axio Observer inverted fluorescence microscope. %BrdU-positive cells were quantified by Image J software (NIH) (n = 6, 2 viewfields per 3 different samples).

Assessment of Myogenesis

ASC myogenesis was evaluated using immunofluorescence staining for early and late stage markers of myogenesis: Pax3/7, Desmin, MyoD1 and MHC.[19] At 3, 7, 14 and 21 days of culture, the samples were fixed as described in "Identification of Proliferating Cells" section, and permeabilized with 0.2% triton X-100 for 10 min. After washing with PBS, samples were incubated with 10% normal donkey serum (Sigma) for 30 min to prevent non-specific binding. The samples were then incubated with one of the following two sets of primary antibodies: (1) rabbit anti-desmin (1:50, Santa Cruz Biotechnology), mouse anti-MyoD1 (1:125, Sigma), or (2) rabbit anti-desmin, goat anti-Pax 3/7 (1:50, Santa Cruz Biotechnology), mouse anti-skeletal myosin (MHC, Sigma, 1:400) diluted in 1% donkey serum at 4 °C overnight. Following this, samples were incubated with corresponding fluorochrome-conjugated secondary antibodies (DyLight649-conjugated donkey anti-rabbit IgG, Cy^{TM}3-conjugated donkey anti-mouse IgG, DyLight488-conjugated donkey anti-goat IgG, 1:200) (Jackson Immunoresearch, West Grove, PA) for 1 h at room temperature. Nuclei were labeled using DAPI. Images were taken using a Zeiss Axio Observer inverted fluorescence microscope and used to quantify number of positively-stained cells using Image J software (n = 6, 2 viewfields per 3 different samples).

Kinetic Stage-Transition Model

We defined stages of cell differentiation based on the expression of the same key myogenic markers determined experimentally (Pax3/7, Desmin, MyoD, MHC). Undifferentiated ASCs were considered Stage 0 (negative in all myogenic markers) and the sequential expression of each marker indicated transition to the subsequent stage (Fig. 1a). Stage 4 was defined as the mature muscle cells positive in all myogenic markers. The changes in cell population in a given stage can occur in two ways: cells either proliferate or die. There are three scenarios of cell proliferation: The parent cell divides either into two daughter cells of the same type (self-renewal), or one daughter cell of the same type and the other being differentiated into a cell of the next stage (asymmetric division), or both daughter cells are differentiated into the cell type of the next stage (Fig. 1b). Thus, in a given stage, the population changes due to cell death and the difference between the numbers of differentiated cells received from the previous state and lost to the next stage (Fig. 1c). The exceptions from this division rule are: (1) Cells do not proliferate in the mature stage, and (2) Differentiated cells are not received in the initial stage.

Such a model of cell transition can be described in terms of three parameters (in general, they are different in each stage and can be affected by the environmental cues), the proliferation rate, p_i (in terms of day^{-1}), death rate, d_i (in terms of day^{-1}), and self-renewal rate, r_i (dimensionless). The latter rate determines the

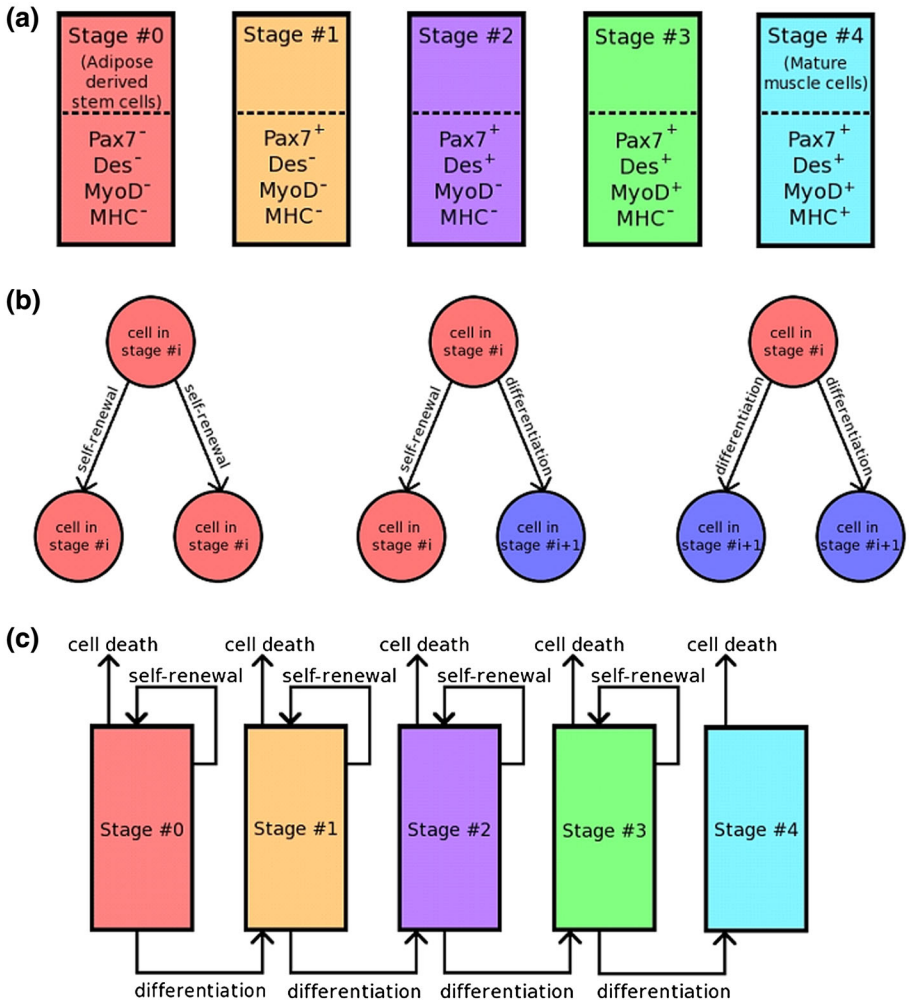

FIGURE 1. (a) Description of stages of ASC myogenic differentiation based on the experimentally determined myogenic markers. (b) Scenarios of cell division during ASC myogenic differentiation. (c) Flowchart of ASC myogenic differentiation with cell transitioning through five major stages.

fraction of self-renewed cells out of all divided cells (thus, the fraction of differentiated cells is $1 - r_i$) where $i = 0, 1, 2, 3, 4$. The balance of changes in the cell number in the five stages under consideration can be written in terms of the following system of kinetic equations:

$$\frac{dn_o}{dt} = (2r_o - 1)p_o n_o - d_o n_o \tag{1}$$

$$\frac{dn_i}{dt} = (2r_i - 1)p_i n_i + 2(1 - r_{i-1})p_{i-1} n_{i-1} - d_i n_i, i = 1, 2, 3 \tag{2}$$

$$\frac{dn_4}{dt} = 2(1 - r_3)p_3 n_3 - d_4 n_4 \tag{3}$$

In each equation, the left-hand side is the change in the number of cells per unit time (the flux), and the right-hand side is the sum of fluxes due to cell dynamics in the corresponding state and connection between the current state with the previous and subsequent stages. In Eq. (2), the first, second, and third terms in the right-hand side describe, (1) the difference between the total number of dividing cells and the number of daughter cells returning (self-renewed) to the current state after division, (2) the number of daughter cells resulting from the division and differentiation in the previous stage, and (3) the number of cells that died in the current stage, respectively. In Eq. (1) describing the initial stage of stem cells, the term associated with cells coming from the previous stage is absent. In Eq. (3) for the final mature state, the terms associated with cell proliferation is absent.

Statistical Analysis

All quantitative experimental results were expressed as mean ± standard deviation. Data was analyzed

with statistically significant values defined as $p < 0.05$ based on one-way analysis of variance (ANOVA) followed by Tukey's *post hoc* test. Statistical significance was set at $p \leq 0.05$. We used the R-squared criterion in the computational fitting of the total number of cells vs. time

RESULTS

Cyclic Stretch Affects ASC Proliferation

Cell proliferation throughout the static and dynamic culture was monitored by measuring the number of metabolically active cells (Fig. 2c). It was observed that the application of uniaxial cyclic strain starting on the third day of culture decreased cell proliferation. On the other hand, the cell number increased steadily during the static culture condition. The proliferation in the dynamic culture decreased significantly between days 3-7 and the difference between the cell numbers were statistically significant on day 7 ($p < 0.05$). The cell numbers remain statistically lower on dynamic culture compared to the static case both on days 14 ($p < 0.01$) and 21 ($p < 0.05$). A similar trend was also observed with the BrdU incorporation study. BrdU immunostaining revealed that the proliferating cells in culture exhibited a random spatial distribution in static cultures at all time points (Fig. 2a). In contrast, the proliferating cells had a tendency to cluster and elongate in the form of tubules in the dynamic case starting from day 7. Counterstaining with DAPI facilitated the quantification of the percent BrdU-positive (%BrdU(+)) cells which correlated with the cell growth patterns observed using the Alamar blue assay (Fig. 2b). The percentage of proliferating cells reached a maximum between days 7 and 14 in static cultures and decreased rapidly after day 14. The application of cyclic strain from day 3 onward in the dynamic cultures caused a sharp decrease in the percentage of cells proliferating between days 3 and 7. The %BrdU(+) cells were significantly higher on days 7 ($p < 0.001$) and 14 ($p < 0.01$) on static case compared to the dynamic. The %BrdU(+) cells remained relatively constant between days 7 and 21 in dynamic culture.

ASCs Express Myogenic Markers with Spatiotemporal Specificity

Immunostaining for early and late myogenic markers (Pax3/7, Desmin, MyoD, MHC) was performed on days 0, 1 (not shown), 3, 7, 14 and 21 for both static and dynamic culture (Fig. 3). The cells were negative for all myogenic markers on day 0. Upon biochemical induction with azacytidine, ASCs express Pax3/7 from as early as day 1. Pax3/7 expression peaked on day 3 and decreased steadily for the remainder of the culture period for both static and dynamic conditions (Fig. 4). Pax 3/7 expression was lower in static relative to dynamic cultures on days 7, 14, and 21 although statistical differences were only detected at day 7 ($p < 0.05$). Cells in both static and dynamic cultures expressed desmin starting from day 3. Following the application of cyclic strain, the percentage of cells expressing desmin was statistically higher in the dynamic compared to static cases ($p < 0.01$ on day 7, $p < 0.001$ on day 14). No statistical differences were observed on day 14. MyoD expression was observed later in the culture. Its frequency was significantly lower in the static culture on days 14 and 21 compared to dynamic samples ($p < 0.001$). Almost all of the cells were MyoD positive on day 21 of the dynamic culture. MHC, a late myogenic marker, was only observed at day 21 with the application of uniaxial cyclic strain. The majority of the cells in the dynamic culture condition were MHC-positive on day 21. This represented a significant increase relative to the static culture group ($p < 0.001$).

Modeling the Kinetics of Multistage ASC Myogenesis

We first estimated the parameters of our model by using the obtained experimental data. The model parameters to be specified were the proliferation, differentiation, and death rates in each stage. The data on the number of cells expressing a particular factor (Fig. 4) were interpreted in terms of combinations of cells being in particular stages. Namely, the number of cells expressing Desmin, MyoD, and MHC, was equal to $n_4 + n_3 + n_2$, $n_4 + n_3$, and n_4, respectively. Then, we used an analytical solution of Eqs. (1)–(3) in terms of exponential functions, which allowed us to effectively adjust the model parameters. Such adjustment of the parameters was qualitatively guided by the experimental data on the number of cells expressing particular factors (Fig. 4b).The relative values of the adjusted parameters were then maintained constant, and the results were obtained based on this set, except the limited use of the experimental data of the total number of cells (Fig. 2c) for scaling all proliferation and self-renewal rates with a single scaling factor. Note that in the static case, the kinetic equations are integrated through the whole time range, while in the dynamic case, the results repeat those in the static case until day 3, and the new initial conditions are used to integrate the system (Eqs. (1)–(3) with the dynamic-case coefficients after that. This approach reflects the experimental conditions of the strain application on day 3. Finally, we assume both n_3 and n_4 equal to zero before day 7 and day 14, respectively, which reflect the absence of MyoD- and MHC-expressing cells in the experiment (Fig. 4b). The resulting parameters for the

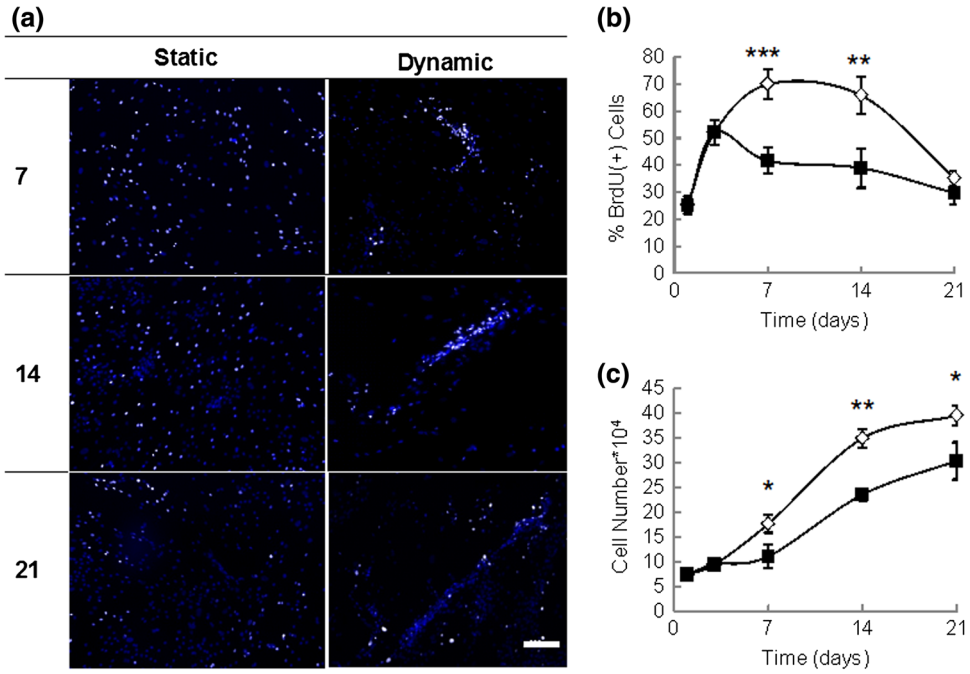

FIGURE 2. (a) Immunofluorescence staining for BrdU (white) and DAPI (blue) for Static and Dynamic culture conditions on days 7, 14 and 21 revealed differences in cell proliferation and organization patterns. Scale bar: 200 μm. (b) Quantification of %BrdU-positive cells in culture using Image J. (c) Viable cell number in culture for static and dynamic culture conditions. Error bars represent standard deviation for $n = 6$. * $p < 0.05$, ** $p < 0.01$, *** $p < 0.001$. ◇: static culture, ■: dynamic culture.

static and dynamic cases are presented in Tables 1 and 2, respectively.

Using our model, we computed various characteristics of ASC myogenesis. First, we present the total number of cells in the static (blue) and dynamic (red) cases. The crosses show the experimental data on days 1, 3, 7, 14, and 21 (Fig. 5a). The R-squared values of the model approximation of the experimental data are equal to 0.832 and 0.948 in the static and dynamic cases, respectively. The number of proliferating cells (per unit time) at any moment of time is shown in Fig. 5b for the static (blue) and dynamic (red) cases. This number, N_p, was computed using the following equation

$$N_p = n_0 p_0 + n_1 p_1 + n_2 p_2 + n_3 p_3 \tag{4}$$

Note that the sharp decrease in N_p for the dynamic culture (Fig. 5b) is related to the switch on day 3 from the parameters used to model static culture to those corresponding to the dynamic case. There are also changes in the slope of N_p in the dynamic case on days 7 and 14 related to such changes in the kinetic graph for stage 3 (Fig. 6b).

Finally, Fig. 5c presents the number (per unit time) of differentiating (transitioning to the next stage), N_d, cells in the static (blue) and dynamic (red) cases. These values were computed by using the equation

$$N_d = n_0 p_0 (1 - r_0) + n_1 p_1 (1 - r_1) + n_2 p_2 (1 - r_2) + n_3 p_3 (1 - r_3) \tag{5}$$

We can also determine separately the numbers of cells per unit time transitioning from one particular stage to the subsequent stage as described in the Discussion below.

The curve showing differentiating cells in dynamic culture (Fig. 5c) has step-wise increases on days 3, 7, and 14.The first one was related to the application of dynamic strains on day 3, the other two are due to the assumed absence of cells in stages 3 and 4 before days 7 and 14, respectively.

In Fig. 6, we present additional information on cell transition between the stages. The left panels (a and c) and the right panels (b and d) present the results for the static and dynamic cases, respectively. Figures 6a and 6b show the kinetics (described by Eqs. (1)–(3)) of the number of cells in each state through day 21. Finally, Figs. 6c and 6d present the distributions of the cells over stages on days 1, 3, 7, 14, and 21. In these figures, the stage composition of the cell population on a particular day and the time evolution of the cell number in each stage can be observed simultaneously.

DISCUSSION

ASCs are an abundant, easily procurable and clinically-relevant cell population[16] that has been successfully differentiated into skeletal muscle albeit with relatively low differentiation efficiency.[13,26,27,39] While

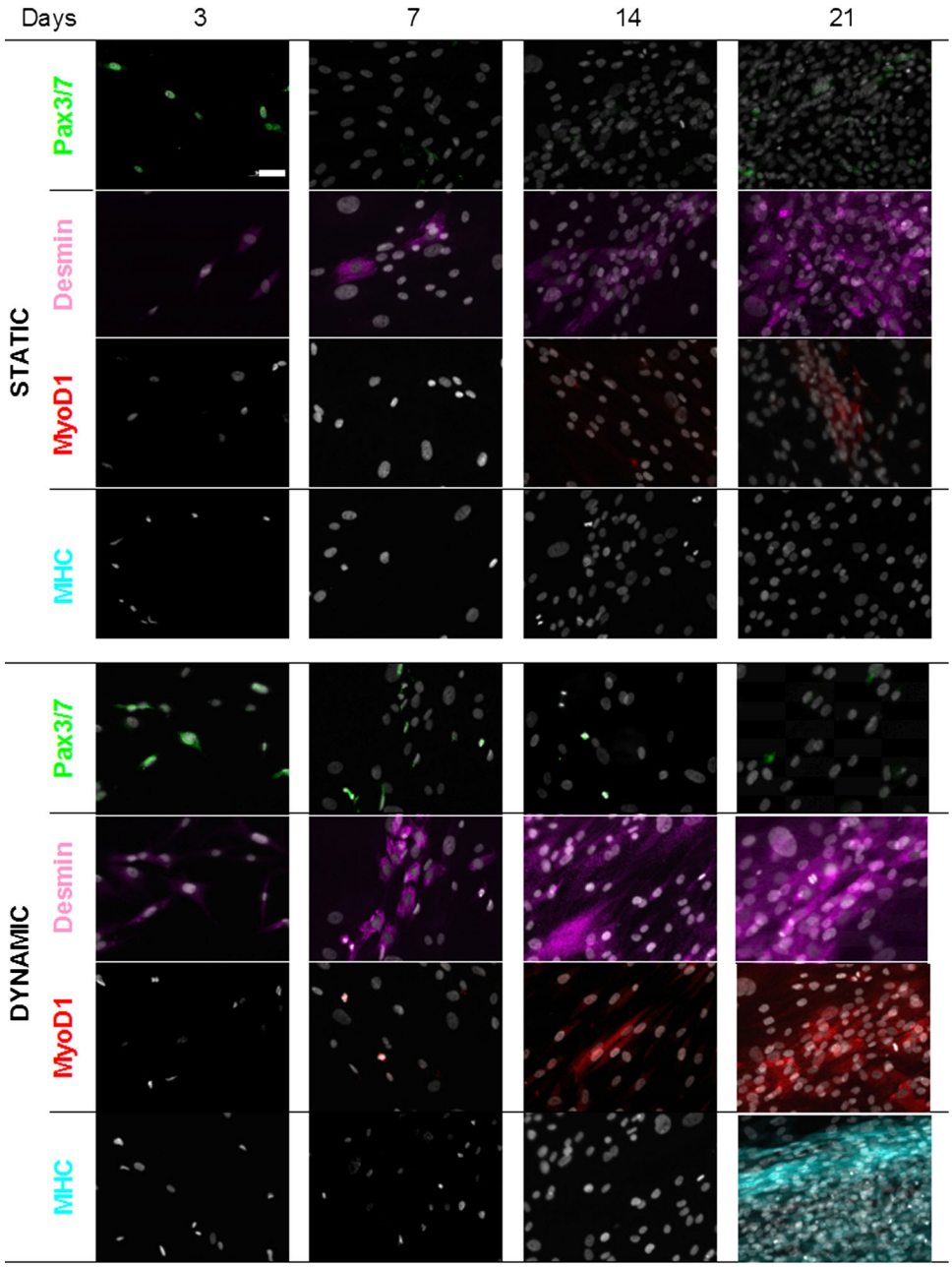

FIGURE 3. Immunofluorescence staining for Pax3/7, Desmin, MyoD and MHC on days 3, 7, 14 and 21 for static and dynamic culture conditions. Expression of myogenic markers were delayed if not inhibited in static culture while ASCs were positive for all myogenic markers on day 21 with the application of dynamic culture. Scale bar: 50 μm.

studies have shown that this efficiency can be improved by growing cells on soft substrates that mimic the muscle microenvironment,[4,5] we have recently found that coordinating the delivery of both biochemical inductive cues and cyclic mechanical strain to ASCs during monolayer cultivation significantly provides robust myogenic differentiation.[37] A closer look into the differentiation process led us to the interesting observation that the temporal expression profile of key transcription factors during ASC myogenesis mimics that of the satellite cell lineage differentiation.[17,33,35] In particular, we have observed sequential expression of Pax3/7, Desmin, MyoD and MHC in our dynamic ASC cultures over the 21 days culture period while they simultaneously undergo significant alignment and multi-nucleation (Figs. 2, 3). The sequential expression of these factors also correlated with the changes in cell morphology: from the original stem cells to aligned

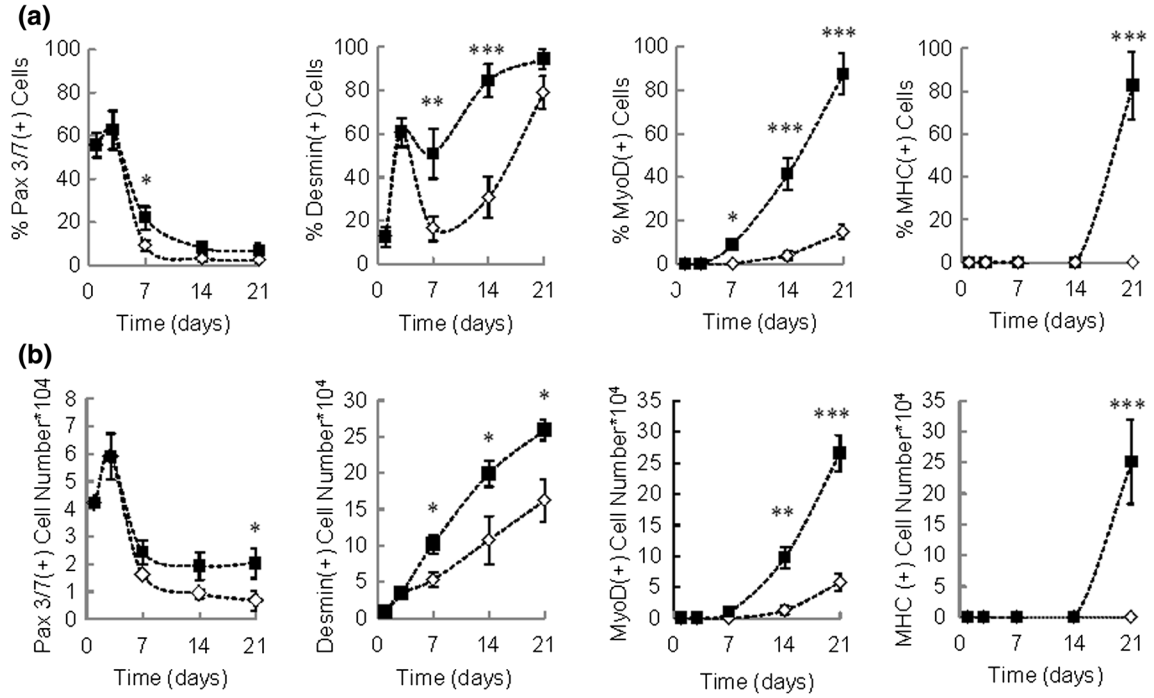

FIGURE 4. Quantification of ASC myogenic marker expression for static and dynamic culture throughout 21 days using Image J based on the immunofluorescence data. (a) % positive-stained cells for myogenic markers. (b) Total number of cells expressing myogenic markers within the culture. Error bars represent standard deviation for $n = 6$. * $p < 0.05$, ** $p < 0.01$, *** $p < 0.001$. ◇: static culture, ■: dynamic culture.

TABLE 1. Static case.

Stage#	0	1	2	3	4
Proliferation rate, *p*	0.43	0.14	0.14	0.14	0.00
Self-renewal rate, *r*	0.80	0.80	0.80	0.50	0.00
Death rate, *d*	0.20	0.20	0.20	0.10	0.08

Estimated model parameters, proliferation, *p* (day^{-1}), self-renewal, *r*, and death *d* (day^{-1}) rates for each stage.

TABLE 2. Dynamic case.

Stage#	0	1	2	3	4
Proliferation rate, *p*	0.14	0.22	0.22	0.22	0.00
Self-renewal rate, *r*	0.60	0.50	0.50	0.50	0.00
Death rate, *d*	0.20	0.10	0.10	0.10	0.08

Estimated model parameters, proliferation, *p* (day^{-1}), self-renewal, *r*, and death rates, *d* day^{-1}) rates for each stage.

myoblasts and, ultimately, fused myotubes. In our experiment cells aligned throughout the membrane by day 14 at an angle of about 30° with respect the direction of stretch.[37] This is in agreement with a similar study employing skeletal muscle cells,[6] where there was a single angle of cell alignment with the mean value close to 35°.

We hypothesized that the expression of each of these markers represented the transition of ASCs from one 'stage' to another and that by understanding the kinetics of cell transition from one stage to another in response to microenvironmental cues, we can provide insight into factors regulating the differentiation process. We therefore, developed a kinetic computational model that correlated experimental parameters with key cellular outcomes. We used the experimentally verified markers to define five discrete stages that characterize ASC differentiation to mature myotubes. By using a series of connected ordinary differential equations, we showed that it was possible to

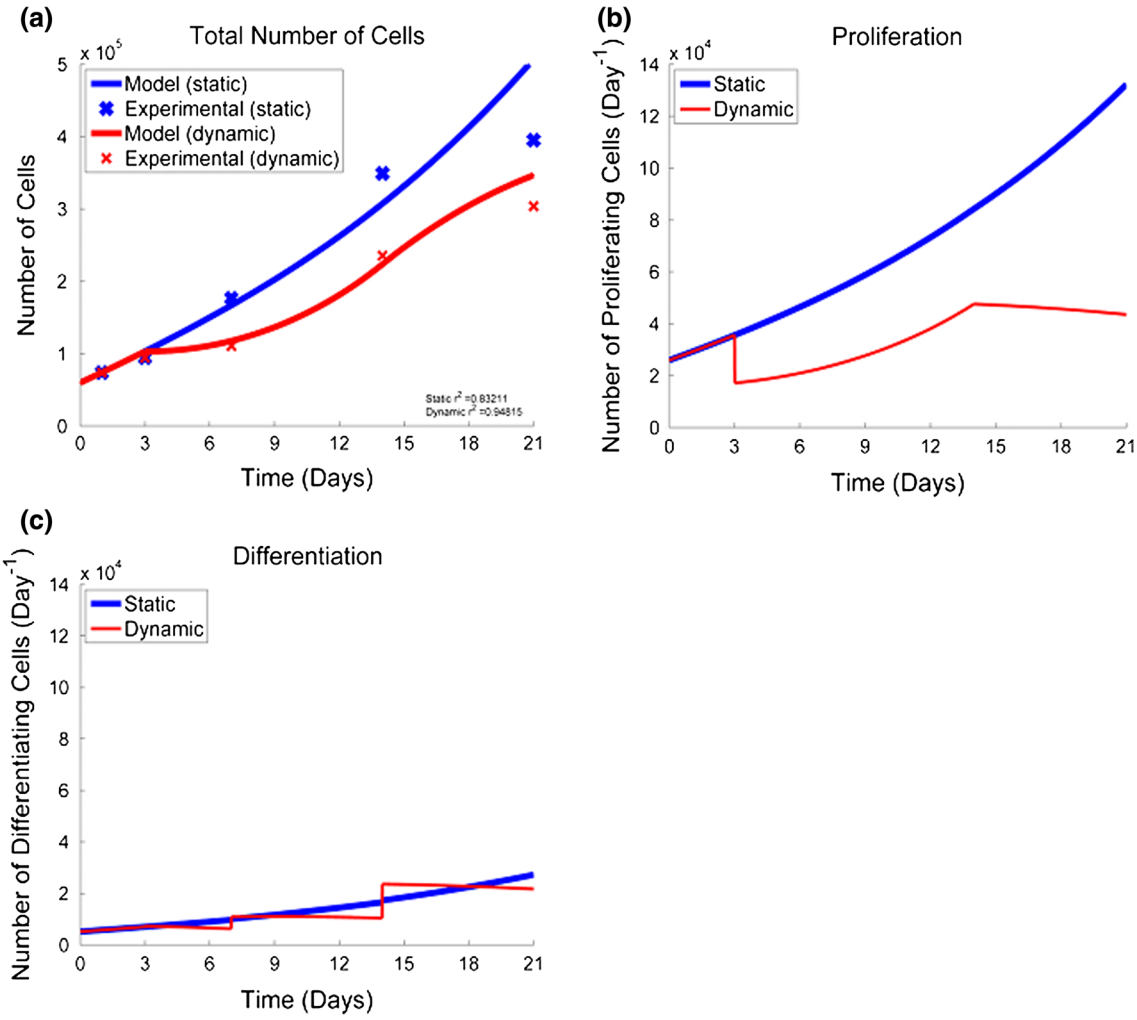

FIGURE 5. Modeling results for the static (blue) and dynamic (red) culture. (a) The total number of cells vs. time. The red and blue crosses show the experimental data for days 1, 3, 7, 14 and 21 days. The *R*-squared values for the modeling approximation are 0.842 and 0.938 in the static and dynamic case, respectively. (b) The total number of proliferating cells vs. time, and (c) The total number of differentiating cells vs. time.

computationally model the kinetics of stage transitions in response to biophysical cues.

In the static case, the computed total number of cells increased with time. This increase was mainly associated with proliferation of cells in the earlier stages. The cells in the later stages also proliferated but they were relatively fewer in number. This is clearly illustrated in Fig. 6c, where the cell composition on day 21 included mostly cells in the first two stages and very few cells in the final stage. In the dynamic case, in contrast, the number of cells in earlier stages decreased and the observed increase in the total number of cells occured mainly because of cell differentiation into the final mature stage. Figures 6c and 6d show the distinctly different cellular compositions on particular days under the two culture conditions. The cell composition on day 21 of dynamic culture had mainly differentiated cells in the mature stage, and a relatively small number of cells remaining in the earlier stages. The computed data in both of the culture conditions (static and dynamic) revealed interesting features in cell transition through the stages. The numbers of total cells as well as proliferating cells were higher under static conditions (Figs. 5a, 5b). The total number of differentiating cells is similar in both conditions (Fig. 5c). Most interestingly, the number of cells transitioning from stage 3 into the final, mature, state 4 in the dynamic case is *an order of magnitude* greater compared to the static case. The number per unit time of cells differentiating into the final stage, N_d^f, is not graphically shown and is computed as $N_d^f = n_s p_3 (1 - r_3)$. The overall kinetics of multistage myogenesis is also different between the two cases. In the static case, the number of cells in all stages increases, including the large numbers and high rates in earlier stages (Fig. 6a). In contrast, in the dynamic case (Fig. 6b), the number of cells in earlier stages decreased,

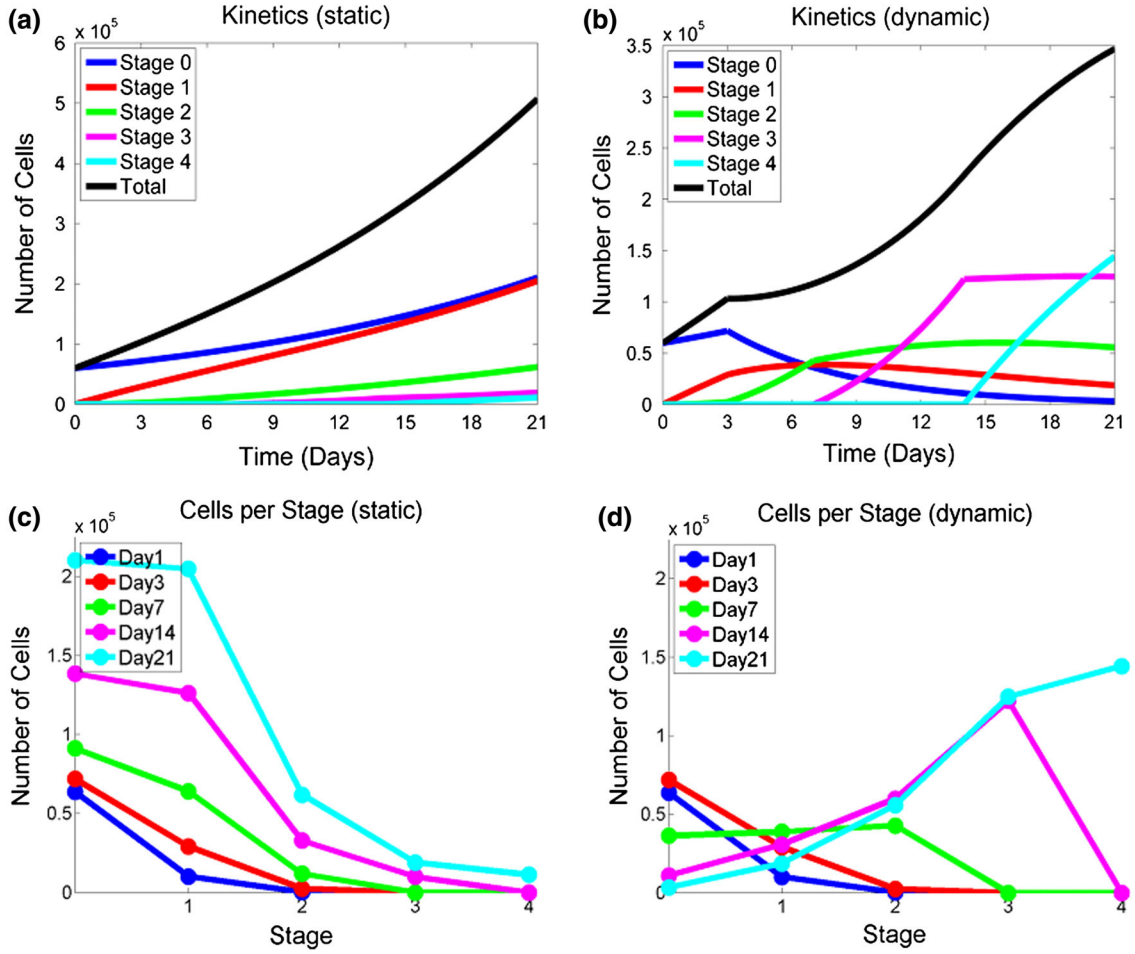

FIGURE 6. Modeling results for the static (a and c) and dynamic (b and d) case. (a) and (b) The number of cells vs. time (kinetics) in each stage. (c) and (d) Cell population distribution over five stages on days 1, 3, 7, 14, and 21.

and the number of cells in mature stage 4 had the highest rate of increase.

In the previous models of stem cell differentiation, the stage progression was necessarily connected to cell proliferation, with differentiation occurring *via* symmetric and asymmetric cell division. Such a mechanism has been proven to be effective in the interpretation and modeling of some type of stem cell differentiation. This mechanism has also been positively viewed in the literature of satellite stem cell differentiation during muscle remodeling.[3] Likewise, cell proliferation occurs during ASC myogenesis and our experiments show an increase in cell number during the progression toward the mature state. Nevertheless, while we do see an increase in the total number of cells, there is no direct evidence that cells proliferate in *each* stage. In this regard, it is possible that cell progression to some stages occur without proliferation, and the right-hand sides of the corresponding kinetic equations should be modified accordingly.

Various types of feedback are common in biological processes. In prior studies, feedback mechanisms have been incorporated in models of stem cell differentiation *via* a sigmoidal or just decreasing function of cell number in the mature state. That modification makes the models nonlinear. We do not have evidence for feedback from the most mature state. However, there is evidence for feedback of a different kind. It has been shown, that the expression of the factor Pax3/7 first increases and then decreases. In the literature, this effect was interpreted as a reciprocal inhibition of Pax7 and MyoD.[29] Thus, we can interpret the decrease in Pax3/7 expression as feedback from stage 3 (MyoD-defined) to stage 1 (Pax3/7-defined). Another type of feedback coming from the later (pre-mature) stages is the observation that differentiation of a stem cell requires the proximity of other cells. This effect can also be described by adding a nonlinear function of the number of cells in the later stages to the kinetic equations of the model.

Our central experimental and modeling observation is that ASC myogenesis is much more effective under dynamic culture conditions in comparison to the static culture. Expression of three factors (Pax3/7, Desmin, and

MyoD) increases by several fold, and that of MHC increases dramatically in the later stage. What would the biological mechanism and corresponding extension of the model be for this? It is known that force (strain) application shifts the energy barriers and corresponding rates of binding for various factors which may explain the higher expression of Pax3/7, Desmin, and MyoD under the strain application. It has been shown in a number of adhered cells that strain application stimulates the cells and corresponding cytoskeletal alignment *via* a rearrangement of FA complexes, the expression of proteins associated with them, and signaling to the cytoskeleton.[2,31] Thus, the latter effect can explain a dramatic increase in MHC, since cell alignment looks as a pre-requisite of further fusion, which is enhanced in clustered and aligned cells. Several studies have explored the effect of passive vs. active mechanical loading on stem cell myogenesis. For example, MSCs seeded in fibrin gels were cultured under 3 different conditions,[28] no strain, constant strain or cyclic strain. Results suggested that active cyclic loading is necessary to obtain smooth muscle phenotype. Therefore, we believe for differentiation towards skeletal muscle lineage (which is an even more active tissue compared to smooth muscle), active mechanical loading is necessary. While these arguments can be used in the explanation and modeling of the strain effect, further studies are required to enlighten optimal dynamic culture conditions to maximize ASC myogenic efficiency.

Our model reproduces a number of features of the experimental data, such as sharp increases in the numbers of cells in stages 3 and 4 on days 7 and 14, respectively. It also provides a quantitative analysis of the effectiveness of the dynamic conditions observed in the experiment. However, the current version of the model does not reproduce some of the quantitative experimental data, e.g., it underestimates the number of cells in the mature state in the dynamic case. Also, the model assumes a relatively homogenous population of ASCs in the initial stage (stage 0). However, various studies have demonstrated that ASCs are heterogenous. It is possible that sub-populations with distinct myogenic potentials exist, but no pro-myogenic populations have yet been identified or characterized for ASCs. Future studies that define this may help to refine the model. Another factor that may impact the model is that the mature state of cells is described as a single stage. However, a more detailed analysis reveals that fusion of myoblasts into a myofiber is a multi-step process which itself can be characterized by expression of additional markers (e.g., Doherty *et al.*[8]). The present model can be extended in terms of a comprehensive parameter optimization algorithm to cover all major features of the experiment as well as modifications of the mathematical formulation to include more characteristic stages and other factors

In summary, the model provides important features of ASC myogenesis, including the total number of cells at any moment of time, changes in the number of cells in each stage as a function of time, the number per unit time of proliferating cells in each state at any time, the number per unit time of differentiating cells in each stage. Finally, the model gives an explanation of the effectiveness of the dynamic conditions in terms of the parameters and characteristics of multistage myogenesis of ASC.

CONCLUSION

ASCs are a clinically-relevant, promising cell source for muscle regenerative therapies that have myogenic differentiation capacity upon biochemical and biophysical stimuli. In this study, we have shown that ASCs express key myogenic markers (Pax3/7, Desmin, MyoD and MHC) with temporal specificity mimicking that of satellite cells under dynamic culture conditions. We developed a compartmental model to describe this process of myogenesis that, complementary to the experiment, reveals a number of features of ASC proliferation and differentiation and helps interpreting the effects of dynamic culture conditions. Ultimately, this model will be used to predict cultivation protocols required to significantly enhance myogenic differentiation of ASCs and to better understand the biological mechanisms such as cell alignment and fusion, cell–cell interactions, and feedback networks involved in ASC myogenesis.

ACKNOWLEDGMENTS

We would like to thank Dr. Jeffrey Gimble for providing the ASCs and Dr. Douglas DiGirolamo for use of the Flexcell system. We also thank Sue Kulason for the computational work at early stages of the project. This work was supported by Maryland Stem Cell Research Fund (2012-MSCRFF-165) and Johns Hopkins Department of Biomedical Engineering.

CONFLICT OF INTEREST

Pinar Yilgor Huri, Andrew Wang, Alexander Spector, and Warren Grayson declare that they have no conflicts of interest.

ETHICAL STANDARDS

Human ASCs were isolated in accordance with an Institutional Review Board approved protocol at the Stem Cell Biology Laboratory, Pennington Biomedical

Research Center. No animal studies were carried out by the authors for this study.

REFERENCES

[1]Asakura, A., M. Komaki, and M. Rudnicki. Muscle satellite cells are multipotential stem cells that exhibit myogenic, osteogenic, and adipogenic differentiation. *Differentiation* 68(4–5):245–253, 2001.

[2]Bershadsky, A. D., N. Q. Balaban, and B. Geiger. Adhesion-dependent cell mechanosensitivity. *Annu. Rev. Cell Dev. Biol.* 19:677–695, 2003.

[3]Charge, S. B., and M. A. Rudnicki. Cellular and molecular regulation of muscle regeneration. *Physiol. Rev.* 84(1):209–238, 2004.

[4]Choi, Y. S., L. G. Vincent, A. R. Lee, M. K. Dobke, and A. J. Engler. Mechanical derivation of functional myotubes from adipose-derived stem cells. *Biomaterials* 33(8):2482–2491, 2012.

[5]Choi, Y. S., L. G. Vincent, A. R. Lee, K. C. Kretchmer, S. Chirasatitsin, M. K. Dobke, and A. J. Engler. The alignment and fusion assembly of adipose-derived stem cells on mechanically patterned matrices. *Biomaterials* 33(29):6943–6951, 2012.

[6]Collinsworth, A. M., C. E. Torgan, S. N. Nagda, R. J. Rajalingam, W. E. Kraus, and G. A. Truskey. Orientation and length of mammalian skeletal myocytes in response to a unidirectional stretch. *Cell Tissue Res.* 302(2):243–251, 2000.

[7]Dingli, D., A. Traulsen, and J. M. Pacheco. Compartmental architecture and dynamics of hematopoiesis. *PLoS ONE* 2(4):e345, 2007.

[8]Doherty, J. T., K. C. Lenhart, M. V. Cameron, C. P. Mack, F. L. Conlon, and J. M. Taylor. Skeletal muscle differentiation and fusion are regulated by the BAR-containing Rho-GTPase-activating protein (Rho-GAP), GRAF1. *J. Biol. Chem.* 286(29):25903–25921, 2011.

[9]Dubois, S. G., E. Z. Floyd, S. Zvonic, G. Kilroy, X. Wu, S. Carling, Y. D. Halvorsen, E. Ravussin, and J. M. Gimble. Isolation of human adipose-derived stem cells from biopsies and liposuction specimens. *Methods Mol. Biol.* 449:69–79, 2008.

[10]Engler, A. J., S. Sen, H. L. Sweeney, and D. E. Discher. Matrix elasticity directs stem cell lineage specification. *Cell* 126(4):677–689, 2006.

[11]Ferrari, G., G. Cusella-De Angelis, M. Coletta, E. Paolucci, A. Stornaiuolo, G. Cossu, and F. Mavilio. Muscle regeneration by bone marrow-derived myogenic progenitors. *Science* 279(5356):1528–1530, 1998.

[12]Galli, R., U. Borello, A. Gritti, M. G. Minasi, C. Bjornson, M. Coletta, M. Mora, M. G. De Angelis, R. Fiocco, G. Cossu, and A. L. Vescovi. Skeletal myogenic potential of human and mouse neural stem cells. *Nat. Neurosci.* 3(10):986–991, 2000.

[13]Geng, J., G. Liu, F. Peng, L. Yang, J. Cao, Q. Li, F. Chen, J. Kong, R. Pang, and C. Zhang. Decorin promotes myogenic differentiation and mdx mice therapeutic effects after transplantation of rat adipose-derived stem cells. *Cytotherapy* 14(7):877–886, 2012.

[14]Goh, B. C., S. Thirumala, G. Kilroy, R. V. Devireddy, and J. M. Gimble. Cryopreservation characteristics of adipose-derived stem cells: maintenance of differentiation potential and viability. *J. Tissue Eng. Regen. Med.* 1(4):322–324, 2007.

[15]Gonda, K., T. Shigeura, T. Sato, D. Matsumoto, H. Suga, K. Inoue, N. Aoi, H. Kato, K. Sato, S. Murase, I. Koshima, and K. Yoshimura. Preserved proliferative capacity and multipotency of human adipose-derived stem cells after long-term cryopreservation. *Plast. Reconstr. Surg.* 121(2):401–410, 2008.

[16]Hutton, D. L., E. M. Moore, J. Gimble, and W. L. Grayson. PDGF and spatiotemporal cues induce development of vascularized bone tissue by adipose-derived stem cells. *Tissue Eng. Part A.* 19(17–18):2076–2086, 2013.

[17]Karalaki, M., S. Fili, A. Philippou, and M. Koutsilieris. Muscle regeneration: cellular and molecular events. *In Vivo* 23(5):779–796, 2009.

[18]Kuang, S., K. Kuroda, F. Le Grand, and M. A. Rudnicki. Asymmetric self-renewal and commitment of satellite stem cells in muscle. *Cell* 129(5):999–1010, 2007.

[19]Le Grand, F., and M. A. Rudnicki. Skeletal muscle satellite cells and adult myogenesis. *Curr. Opin. Cell Biol.* 19(6):628–633, 2007.

[20]Lee, W. C., T. M. Maul, D. A. Vorp, J. P. Rubin, and K. G. Marra. Effects of uniaxial cyclic strain on adipose-derived stem cell morphology, proliferation, and differentiation. *Biomech. Model. Mechanobiol.* 6(4):265–273, 2007.

[21]Li, Y., and J. Huard. Differentiation of muscle-derived cells into myofibroblasts in injured skeletal muscle. *Am. J. Pathol.* 161(3):895–907, 2002.

[22]Liu, C., S. Baek, J. Kim, E. Vasko, R. Pyne, and C. Chan. Effect of static pre-stretch induced surface anisotropy on orientation of mesenchymal stem cells. *Cell. Mol. Bioeng.* 7(1):106–121, 2014.

[23]Liu, G., H. Zhou, Y. Li, G. Li, L. Cui, W. Liu, and Y. Cao. Evaluation of the viability and osteogenic differentiation of cryopreserved human adipose-derived stem cells. *Cryobiology* 57(1):18–24, 2008.

[24]Marciniak-Czochra, A., T. Stiehl, A. D. Ho, W. Jager, and W. Wagner. Modeling of asymmetric cell division in hematopoietic stem cells—regulation of self-renewal is essential for efficient repopulation. *Stem Cells Dev.* 18(3):377–385, 2009.

[25]Maul, T. M., D. W. Chew, A. Nieponice, and D. A. Vorp. Mechanical stimuli differentially control stem cell behavior: morphology, proliferation, and differentiation. *Biomech. Model. Mechanobiol.* 10(6):939–953, 2011.

[26]Meligy, F. Y., K. Shigemura, H. M. Behnsawy, M. Fujisawa, M. Kawabata, and T. Shirakawa. The efficiency of in vitro isolation and myogenic differentiation of MSCs derived from adipose connective tissue, bone marrow, and skeletal muscle tissue. *In Vitro Cell Dev. Biol. Anim.* 48(4):203–215, 2012.

[27]Mizuno, H., P. A. Zuk, M. Zhu, H. P. Lorenz, P. Benhaim, and M. H. Hedrick. Myogenic differentiation by human processed lipoaspirate cells. *Plast Reconstr. Surg.* 109(1):199–209; discussion 210–191, 2002.

[28]Nieponice, A., T. M. Maul, J. M. Cumer, L. Soletti, and D. A. Vorp. Mechanical stimulation induces morphological and phenotypic changes in bone marrow-derived progenitor cells within a three-dimensional fibrin matrix. *J. Biomed. Mater. Res. A* 81(3):523–530, 2007.

[29]Olguin, H. C., Z. Yang, S. J. Tapscott, and B. B. Olwin. Reciprocal inhibition between Pax7 and muscle regulatory factors modulates myogenic cell fate determination. *J. Cell Biol.* 177(5):769–779, 2007.

[30]Powell, C. A., B. L. Smiley, J. Mills, and H. H. Vandenburgh. Mechanical stimulation improves tissue-engineered human skeletal muscle. *Am. J. Physiol. Cell Physiol.* 283(5):C1557–1565, 2002.

[31]Qian, J., H. Liu, Y. Lin, W. Chen, and H. Gao. A mechanochemical model of cell reorientation on substrates under cyclic stretch. *PLoS ONE* 8(6):e65864, 2013.
[32]Quintero, A. J., V. J. Wright, F. H. Fu, and J. Huard. Stem cells for the treatment of skeletal muscle injury. *Clin. Sports Med.* 28(1):1–11, 2009.
[33]Shi, X., and D. J. Garry. Muscle stem cells in development, regeneration, and disease. *Genes Dev.* 20(13):1692–1708, 2006.
[34]Sicari, B. M., C. L. Dearth, and S. F. Badylak. Tissue engineering and regenerative medicine approaches to enhance the functional response to skeletal muscle injury. *Anat. Rec. (Hoboken).* 297(1):51–64, 2014.
[35]Wagers, A. J., and I. M. Conboy. Cellular and molecular signatures of muscle regeneration: current concepts and controversies in adult myogenesis. *Cell* 122(5):659–667, 2005.
[36]Wong, S. T., S. K. Teo, S. Park, K. H. Chiam, and E. K. Yim. Anisotropic rigidity sensing on grating topography directs human mesenchymal stem cell elongation. *Biomech. Model. Mechanobiol.* 13(1):27–39, 2014.
[37]Yilgor Huri, P., C. A. Cook, D. L. Hutton, B. C. Goh, J. M. Gimble, D. J. DiGirolamo, and W. L. Grayson. Biophysical cues enhance myogenesis of human adipose derived stem/stromal cells. *Biochem. Biophys. Res. Commun.* 438(1):180–185, 2013.
[38]Zandstra, P. W., D. A. Lauffenburger, and C. J. Eaves. A ligand-receptor signaling threshold model of stem cell differentiation control: a biologically conserved mechanism applicable to hematopoiesis. *Blood* 96(4):1215–1222, 2000.
[39]Zuk, P. A., M. Zhu, H. Mizuno, J. Huang, J. W. Futrell, A. J. Katz, P. Benhaim, H. P. Lorenz, and M. H. Hedrick. Multilineage cells from human adipose tissue: implications for cell-based therapies. *Tissue Eng.* 7(2):211–228, 2001.